

# Enhanced field-of-view integral imaging display using multi-Köhler illumination

Ángel Tolosa,<sup>1,\*</sup> Raúl Martínez-Cuenca,<sup>2</sup> Héctor Navarro,<sup>3</sup> Genaro Saavedra,<sup>3</sup>  
Manuel Martínez-Corral,<sup>3</sup> Bahram Javidi,<sup>4,5</sup> and Amparo Pons<sup>3</sup>

<sup>1</sup>AIDO, Technological Institute of Optics, Color and Imaging, E-46117 Paterna, Spain

<sup>2</sup>Department of Mechanical Engineering and Construction, Univeritat Jaume I, E-12071 Castelló, Spain

<sup>3</sup>Department of Optics, University of Valencia, E-46100 Burjassot, Spain

<sup>4</sup>Electrical and Computer Eng Dept., Univ. of Connecticut, Storrs, Connecticut 06269, USA

<sup>5</sup>Bahram.Javidi@UConn.edu

\*atolosa@aido.es

**Abstract:** A common drawback in 3D integral imaging displays is the appearance of pseudoimages beyond the viewing angle. These pseudoimages appear when the light rays coming from each elemental image are not passing through the corresponding microlens, and a set of barriers must be used to avoid this flipping effect. We present a pure optical arrangement based on Köhler illumination to generate these barriers thus avoiding the pseudoimages. The proposed system does not use additional lenses to project the elemental images, so no optical aberrations are introduced. As an added benefit, Köhler illumination provides a higher contrast 3D display.

©2014 Optical Society of America

**OCIS codes:** (110.4190) Multiple imaging; (110.6880) Three-dimensional image acquisition.

---

## References and links

1. F. Okano, H. Hoshino, J. Arai, and I. Yuyama, "Real-time pickup method for a three-dimensional image based on integral photography," *Appl. Opt.* **36**(7), 1598–1603 (1997).
2. G. Lippmann, "Epreuves reversibles donnant la sensation du relief," *J. Phys.* **7**, 821–825 (1908).
3. H. E. Ives, "Optical properties of a Lippman lenticulated sheet," *J. Opt. Soc. Am. A* **21**(3), 171 (1931).
4. C. B. Burckhardt, "Optimum Parameters and Resolution Limitation of Integral Photography," *J. Opt. Soc. Am. A* **58**(1), 71–74 (1968).
5. J. Arai, F. Okano, M. Kawakita, M. Okui, Y. Haino, M. Yoshimura, M. Furuya, and M. Sato, "Integral Three-Dimensional Television Using a 33-Megapixel Imaging System," *J. Disp. Technol.* **6**(10), 422–430 (2010).
6. J. Y. Son, S. H. Kim, D. S. Kim, B. Javidi, and K. D. Kwack, "Image-forming principle of integral photography," *J. Disp. Technol.* **4**(3), 324–331 (2008).
7. F. Okano, J. Arai, K. Mitani, and M. Okui, "Real-time integral imaging based on extremely high resolution video system," *Proc. IEEE* **94**(3), 490–501 (2006).
8. S. H. Hong, J. S. Jang, and B. Javidi, "Three-dimensional volumetric object reconstruction using computational integral imaging," *Opt. Express* **12**(3), 483–491 (2004).
9. R. Martínez-Cuenca, G. Saavedra, M. Martínez-Corral, and B. Javidi, "Progress in 3-d multiperspective display by integral imaging," *Proc. IEEE* **97**(6), 1067–1077 (2009).
10. S. H. Hong and B. Javidi, "Three-dimensional visualization of partially occluded objects using integral imaging," *J. Disp. Technol.* **1**(2), 354–359 (2005).
11. M. Martínez-Corral, B. Javidi, R. Martínez-Cuenca, and G. Saavedra, "Multifacet structure of observed reconstructed integral images," *J. Opt. Soc. Am. A* **22**(4), 597–603 (2005).
12. H. Choi, S. W. Min, S. Jung, J. H. Park, and B. Lee, "Multiple-viewing-zone integral imaging using a dynamic barrier array for three-dimensional displays," *Opt. Express* **11**(8), 927–932 (2003).
13. J. Arai, F. Okano, H. Hoshino, and I. Yuyama, "Gradient-index lens-array method based on real-time integral photography for three-dimensional images," *Appl. Opt.* **37**(11), 2034–2045 (1998).
14. R. Martínez-Cuenca, A. Pons, G. Saavedra, M. Martínez-Corral, and B. Javidi, "Optically-corrected elemental images for undistorted Integral image display," *Opt. Express* **14**(21), 9657–9663 (2006).
15. A. Tolosa, R. Martínez-Cuenca, A. Pons, G. Saavedra, M. Martínez-Corral, and B. Javidi, "Optical implementation of micro-zoom arrays for parallel focusing in integral imaging," *J. Opt. Soc. Am. A* **27**(3), 495–500 (2010).
16. S. Jung, J.-H. Park, H. Choi, and B. Lee, "Viewing-angle-enhanced integral three-dimensional imaging along all directions without mechanical movement," *Opt. Express* **11**(12), 1346–1356 (2003).

17. N. Davies, M. McCormick, and L. Yang, "Three-dimensional imaging systems: a new development," *Appl. Opt.* **27**(21), 4520–4528 (1988).
  18. J. Arai, H. Kawai, and F. Okano, "Microlens arrays for integral imaging system," *Appl. Opt.* **45**(36), 9066–9078 (2006).
  19. R. Martínez-Cuenca, H. Navarro, G. Saavedra, B. Javidi, and M. Martínez-Corral, "Enhanced viewing-angle integral imaging by multiple-axis telecentric relay system," *Opt. Express* **15**(24), 16255–16260 (2007).
  20. R. Martínez-Cuenca, G. Saavedra, A. Pons, B. Javidi, and M. Martínez-Corral, "Facet braiding: a fundamental problem in integral imaging," *Opt. Lett.* **32**(9), 1078–1080 (2007).
- 

## 1. Introduction

Integral Imaging (InIm) has generated great interest in the last decades given its ability to produce full three-dimensional (3D) images of a scene [1]. It is based on the integral photography, a technique proposed by Lipmann in 1908 as a way to record and project 3D images under incoherent or ambient light with both horizontal and vertical parallax [2]. As in holography, integral photography recovers the direction and intensity of the rays of the captured scene, so the 3D images projected are autostereoscopic and there is no need for using special glasses for 3D visualization [3,4]. InIm follows the same optical principles as Lipmann's proposal but taking profit of the power of modern digital techniques, which combine digital capture and display with computational imaging [5–9].

InIm systems can be used to record and display 3D images. In the recording stage, a microlens array (MLA) provides with a single snapshot an array of microimages of the scene, which are recorded by an electronic sensor in a unique 2D image called integral image (II). Every microimage, also called elemental image (EI), contains its own perspective of the scene as it has been taken from the point of view of the corresponding microlens (ML), so the 3D information of the scene is encoded through the elemental images in the integral image. The 3D information can be decoded either by computational or optical methods. Computational processing provides a set of powerful tools to extract rich 3D content from the II in contrast to conventional 2D images. For example, it is possible to obtain depth information of the objects in the scene, to focus on planes chosen at will and to generate an all in focus image from a stack of focused planes [8, 9], or to erase artifacts in order to get sharp images of partially-occluded objects [10]. Optical reconstruction exploits the principle of reversibility of the rays to recover the 3D scene from the II. For 3D display, the MLA is placed in front of the II and thus each elemental image is projected onto the image plane of the corresponding microlens. When a camera is placed in front of the MLA a perspective of the 3D image is observed. Since each part of the scene is provided by a different microlens, the generation of the 3D perspectives is actually a multifaceted process [11]. Human observers will see slightly different perspective of the reconstructed image through each eye, thus providing the sensation of relief. The field of view (FOV) is determined by the parameters of projection. There is a set of perspectives that can be observed, and the 3D image is visualized as a true 3D image, with depth and parallax.

The use of arrays of microlenses for capturing or projecting integral images gives the InIm technique two major drawbacks. In the capture stage, an overlap between neighboring microimages occurs when the size of the microimage exceeds the pitch of the MLA (i.e., the distance between the centers of microlenses). This overlapping can be solved by placing a set of physical barriers to divide the sensor in a set of separate elemental cells, as in [12], where a dynamic barrier array is also used to increase the range of perspective of the 3D image. Since this method requires complex manufacturing techniques, several methods have been proposed to implement the barriers optically; for example, by using a set of gradient-index lens-array [13], by means of a telecentric relay system (TRES) [14, 15] or by using switching polarizing masks [16]. In the viewing stage a similar situation happens when the observer looks at the MLA far from the optical axis. For on axis observation, each facet is obtained when the observer sees a microimage through the corresponding microlens. However, for high observation angles the FOV of the 3D display is exceeded and the facet provided by a

microlens may come from a microimage not located right in front of it. Under these conditions, a flipped image (or pseudoimage) is obtained. Again, a set of physical barriers can be used to solve the problem, but little research has been done to implement the barriers optically up to now. An autocollimating screen was proposed to build optical barriers [17], but the system was exceedingly complex and sensitive to aberrations and misalignments. Other methods employ a setup of GRIN lenses or an array of three convex microlenses to generate orthoscopic images and implement the barriers [18]. The MATRES method uses three telecentric relay systems to generate the barriers and increase the range of perspective [19], but the system presents low light efficiency, as it requires the use of a small pinhole. Up to now there is no system that provides optical barriers for conventional MLAs in the display stage.

In this paper, we present the demonstration of an efficient optical arrangement to implement optical barriers in 3D integral imaging displays and thus avoiding the flipping effect. The proposed 3D display uses a multi-Köhler illuminating system based on the use of only one additional MLA and a field lens. This use of Köhler illumination does not cause additional aberrations as it serves only to illuminate the EIs. Also, the standard configuration of II-MLA is respected. Furthermore, the use of Köhler illumination provides a uniform illumination for the elemental images, so the observed images exhibit more uniform aspect and higher contrast. The paper is structured as follows: In Section 2, we introduce the principles of integral imaging capture, display and visualization. We also analyze the origin of the flipping effect. Next, we recall the basics of Köhler illumination in Section 3. Section 4 is devoted to the description of the system implementing the optical barriers for the 3D display. Finally, we demonstrate the performance of the proposed system with experiments in Section 5.

## 2. Principles of integral imaging

The process of observing a 3D autostereoscopic image on the basis of an integral imaging system can be separated into three main steps: the pickup of the integral image, the projection stage, and the visualization as described in the following subsections.

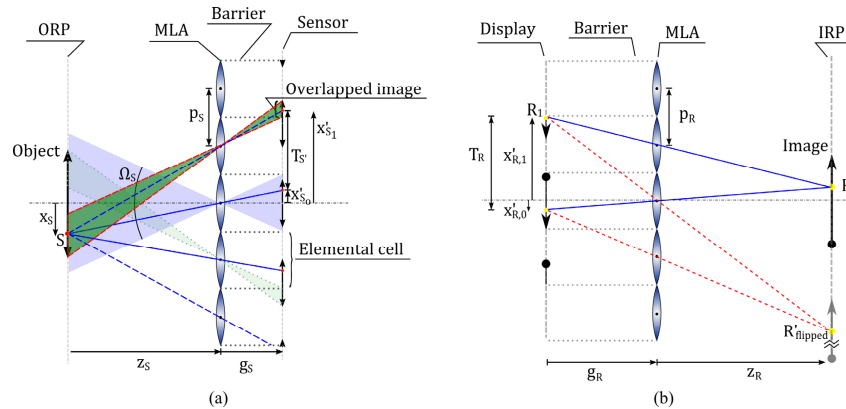


Fig. 1. Capturing (a) and display (b) of integral images. The rays of light go from left to right.

### 2.1 3-D image pickup stage

In the pickup stage, a MLA projects on an image sensor a 2D image composed of a set of microimages of the 3D scene. Each one of these microimages is the result of projecting the incoming light through the corresponding microlens in the MLA. The 2D image with the array of microimages is called integral image and encodes between the set of microimages the direction and intensity of the light coming from the scene and therefore stores the three dimensional information of the scene. A schematic system for capturing an integral image is

shown in Fig. 1(a). During the pickup process, the light beams scattered (or emitted) by each point  $S$  on the surface of an extended object pass through a MLA and provide a set of microimages  $\{S'_n\}$ . If we choose the center of one microlens as the coordinate origin, the lateral coordinate for the image point for the  $n$ -th microimage will be given by

$$x'_{S',n} = \frac{g_S}{z_S}(np_S - x_S) + np_S, \quad (1)$$

where  $(x_S, z_S)$  are the coordinates of the source point  $S$ ,  $g_S$  is the capture distance between the plane of sensor and the lens array, and  $p_S$  is the distance between the centers of the microlenses (pitch). If the coordinate  $z_S$  satisfies the thin lens law  $1/z_S + 1/g_S = 1/f$ , the microimage will appear focused on the sensor. This in-focus plane is called object reference plane (ORP).

In Fig. 1(a), the space on the sensor has been separated by means of a set of parallel barriers into a set of elemental cells. Each cell is located just in front of the corresponding microlens, where the microimage will be recorded. These barriers are needed to limit the extension of the microimages, which cannot be greater than the pitch between MLs. If the extension of the microimages were greater than the pitch, the images provided by neighboring microlenses would overlap and the information will be lost. The barriers fit the size of the EIs and hence the FOV of the MLs, which is determined by the angle  $\Omega_S$ . The FOV of the integral imaging display, defined as the maximum range of perspectives that can be observed, will be related to this angle.

### 2.2 3-D image projection

The display stage recovers the 3D information of the scene from the II. As schematized in Fig. 1(b), the optical display consists of the projection of the integral image through the MLA, which is placed in front of the display. Now the microimages  $\{S'_n\}$  will act as micro-sources  $\{R\}$ , which will provide light rays that intersect after the MLA in the reconstructed point  $R'$ , with coordinates:

$$x_{R'} = \frac{p_R}{T_R - p_R} x'_{R_0}, \quad (2)$$

$$z_{R'} = \frac{p_R}{T_R - p_R} g_R, \quad (3)$$

where  $x'_{R_0}$  is the lateral coordinate of  $R$  for the microlens chosen as origin of coordinates,  $T_R$  is the constant pitch between equivalent points  $R$  at each elemental image,  $p_R$  is the pitch of the array of the ML, and  $g_R$  is the distance between the integral image and the MLA.

Given that the location of the reconstruction points depends on the geometry of the system, the displayed image can be distorted with respect to the original scene if reconstruction parameters are not chosen carefully. A homogeneous scaling of all the geometrical parameters provides a homogeneous scaling of the displayed scene.

Finally, note that the light rays coming from the  $n$ -th microimage will pass through all the microlenses, generating multiple reconstruction paths. In order to enable only one reconstruction point, a set of barriers must be used to block the rays crossing from the  $n$ -th micro-source to the neighboring microlens.

### 2.3 3-D viewing of the scene

In the viewing stage, an observer is placed in front of the InIm display. The image formed on the sensor is the result of a multifacet process [11], and its quality can be strongly influenced

by the facet braiding, which causes an out of focus degraded structure on the image planes [20]. This process is based on the vignetting between the microlenses borders and the aperture stop of the observer lens, which limits the field of the reconstructed scene viewed through each microlens.

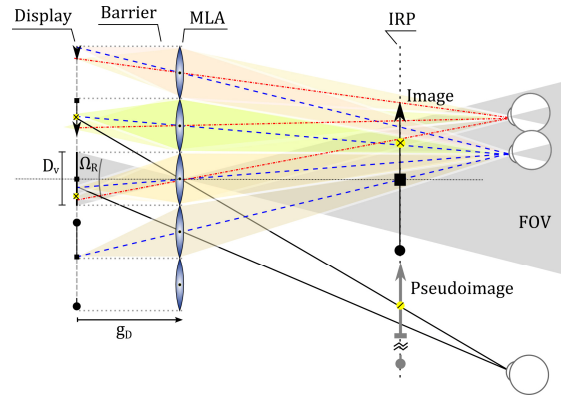


Fig. 2. Visualization of 3D images through a 3D display based on integral imaging.

As we schematize in Fig. 2, an observer placed in front of the MLA to see the reconstructed image will see a different portion of the image through each lenslet. The image visualized is formed by the combination of these facets onto the retina. When the observer moves in a plane parallel to the MLA, it changes the point of view of the reconstructed image, since the facets forming the image are observed through neighboring microlenses and hence with a different perspective. The range of perspectives of the 3D display is given by the angle

$$\Omega_R = 2 \arctan \left( \frac{D_v}{2g_D} \right), \quad (4)$$

where  $D_v$  is the size of the elemental image in the display projected by the MLs, and  $g_D$  is the distance between the display and the MLs. During the viewing, a human observer moving in a plane parallel to the MLA will see the object with full horizontal and vertical parallax. This happens over a certain FOV, which determines the actual range of perspectives of the 3D display. According to Eq. (4), the setting angle of the FOV depends on the size of the elemental images, which we usually set equal to the pitch of the microlenses. As can be seen in Fig. 2, beyond this angle the observer is out of the FOV and it is impossible to view another perspective of the reconstructed object. What is viewed is a jump in the 3D image, and a new ghost image appears as a result of viewing pixels of the neighboring elemental images through the microlenses that are not placed in front of them. To avoid these undesirable ghost images, it is possible to place optical or physical barriers, as in the capture stage, to block the rays that come from an EI with angles higher than  $\Omega_R$ .

### 3. Importance of illumination systems: Köhler illumination

The design of proper illumination systems is important for most optical systems. An inappropriate illumination may affect the contrast of the images (as in conventional photography), reduce their resolution (as in optical microscopy) or even destroy the image itself (as in holography). Various illumination techniques have been developed in order to improve the performance of optical systems such as super resolution by structured illumination or the use of Köhler illumination in microscopy.

The Köhler configuration was designed to avoid the problems associated with critical illumination in microscopy. In critical illumination, the light source is imaged onto the sample, so the inhomogeneities of the source itself superimpose the structure of the sample.

Conversely, as is shown schematically in Fig. 3(a) where the typical path for transmission microscopy has been depicted, in Köhler illumination the image of the source is formed at infinity. It means that a set of parallel rays homogeneously illuminates the specimen. Köhler illumination continues to be the optimum method of illumination in microscopy.

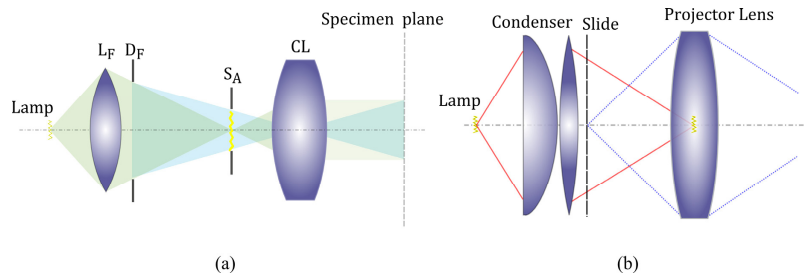


Fig. 3. (a) Köhler illumination path in transmission microscopy and (b) in slide projection.

To understand this system we note in Fig. 3(a) that the standard microscope for transmission has a collector lens,  $L_F$ , which focuses the source on the front focal plane of a condenser lens. Because this image is on its object focal plane, the condenser lens images the source at infinity generating a bundle of parallel rays that illuminates uniformly any plane on the back side. A diaphragm,  $S_A$ , on the front focal plane of the condenser acts as aperture stop and controls the angle of the cone of parallel rays reaching the specimen plane, and hence the lighting level on the sample. A diaphragm,  $D_F$ , placed behind the lens  $L_F$  acts as field stop and controls the illuminating field on the specimen plane without changing the illuminating level. To avoid vignetting, the distance of this stop is adjusted to be conjugated with the specimen plane through the condenser lens, being focused together with the specimen on the observer image plane. Since the image planes of the source through the different lenses of the microscope including objective and observer, and the images planes of the specimen follow different paths, the source will be defocused on the observer image plane, and the image of the sample will exhibit high contrast.

This kind of illumination was adapted to be used in slide projection systems, cinema projectors or micro photolithography, as schematized in Fig. 3(b). In this configuration, the slide is not illuminated with parallel rays, and the angle of illumination and the size of the illuminated field on the slide plane are both fixed by the condenser. However, the slide is uniformly illuminated as it is placed close to the condenser and the lamp is imaged into the entrance pupil of the projection lens.

#### 4. Principle of parallel illumination

As stated in Section 2, physical barriers are introduced to block the passage of light rays departing from a given elemental image through the neighboring lenslets. The principle of optical illumination barriers proposed in this paper aims at impeding this undesirable crossing by using an illumination pattern such that all the light rays emerging from any point within any elemental image pass through the aperture of the corresponding microlens. In order to show how to achieve such illumination pattern, we start by analyzing the conditions that hold when a single pair elemental image - lenslet is considered. Then, we show a simple optical design to achieve this kind of illumination on every elemental image by using only one light source and an additional MLA. For the sake of completeness, we finally demonstrate that the use of a matrix of sources does not work.

The simple setup shown in Fig. 4(a) serves to illustrate the form of the required illumination pattern for a single EI and its corresponding microlens. Here, a plane object  $O$  is illuminated in such a way that the size of the illuminated field,  $\phi_0$ , coincides with the size of the imaging lens,  $L$ , which is placed in front of the object at a distance  $g$ . In this figure,  $O(x)$  represents a point of the integral image; the part of  $O$  that is actually illuminated coincides

with one of the elemental images; and  $L$  represents the corresponding microlens. Note that the extent of the cone of rays emitted by any object point  $O(x)$  is limited by the lens aperture, which is the condition for the optical illumination barriers. We may summarize the process for an appropriate implementation of the optical illumination barriers by setting the following three fundamental conditions: a) the size of the illuminated field must be similar to the size of the elemental image, b) the diameter of the cone of rays on the plane of the microlens must match the microlens pitch, and c) the central ray of the cone must be directed towards the center of the corresponding microlens.

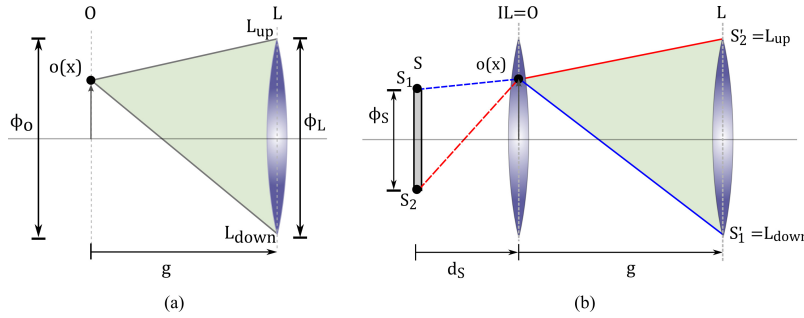


Fig. 4. (a) The conditions needed for optical barriers which are accomplished by a Köhler illumination system. (b) A simple method to provide an illuminating field onto a plane object that verifies the conditions in (a).

Figure 4(b) shows a simple method to provide an illuminating field onto a plane object that verifies these three conditions. In this setup, a light source  $S$  of size  $\phi_s$  is imaged onto the plane containing  $L$  by using an illuminating lens,  $IL$ . The object  $O$  is located just in the plane containing  $IL$ . As the size of the illuminated field is simply the size of the  $IL$ ,  $\phi_L = \phi_L$  ensures the accomplishment of the first condition. Condition (b) is accomplished as long as the light source is imaged onto the plane  $L$  and its size verifies the condition

$$\phi_s = \frac{d_s}{g} \phi_L . \quad (5)$$

The ray tracing in the figure has been done under this condition, so the point  $S_1$  in the source plane is imaged onto the point  $S_1'$ , which coincides with  $L_{down}$ . Also, the point  $S_2$  is imaged onto the upper border of  $L$ ,  $L_{up}$ . Thus, it is easy to verify that the ray  $S_1O(x)S_1'$  provides the upper limit of the cone of rays emitted from  $O(x)$ , that is,  $O(x)L_{up}$ . By following the path of the ray  $S_2O(x)S_2'$  one gets the bottom limit of this cone of rays  $O(x)L_{down}$ . Therefore, the diameter of the cone of rays equals the lens diameter to satisfy condition b). Also, this ray tracing clearly shows that all the rays emerging from  $O(x)$  fall within the lens aperture, so the central ray of the cone passes through the lens center to satisfy condition c). Hence making the image of the source coincident with  $L$  directly ensures conditions (b) and (c) are satisfied.

In order to apply the optical illumination barrier principle to an integral imaging system, each elemental image should be illuminated with a system equivalent to that in Fig. 4(b). Now, the object is replaced by the  $i$ -th elemental image, the  $IL$  must be replaced by  $i$ -th lenslet in a first MLA, which will be named as the illuminating MLA or IMLA, and the imaging lens by the  $i$ -th lenslet in a second MLA, which will be named as projection MLA or PMLA. Note that the design shown in Fig. 5(a) is able to provide a set of optical illumination barriers onto the plane of the integral image in the MLA. If one concentrates on the  $i$ -th lenslet element, only the  $i$ -th elemental image is illuminated by the lenslet  $j$ . With a proper setting for the source size and the distances  $d_s$  and  $g$ , the source is imaged onto the MLA

plane with the same size as the lenslet. Finally, the axis of the illumination cone passes through the lenslet center. However, if one concentrates on the element  $i + 1$ , it is straightforward to note that the axis of the cone of rays is not directed towards the axis of the  $i + 1$ -th lenslet. In other words, the multiple images of  $S$  have a proper size, but only the one provided by the central element is actually coincident with the corresponding lenslet  $PL_i$ . This would cause the formation of pseudoimages as the rays from the  $i + 1$  elemental image pass through the  $i + 2$  lenslet.

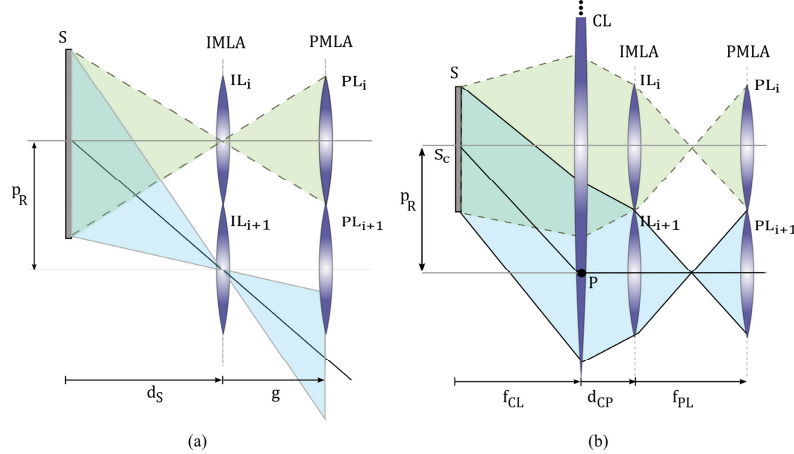


Fig. 5. Using a MLA to replicate Köhler illumination onto each elemental image: (a) light cones do not fill the PMLA properly and will lead to flipping effect; (b) correct illumination avoids flipping by filling the PMLA properly.

The system in Fig. 5(b) overcomes this problem by using a telecentric relay system to match the multiple images of  $S$  with the corresponding microlenses. Here, the light source is placed in the front focal plane of a collimating lens  $CL$ , so the image of the source through the lenses  $CL$  and  $IL$  is located at the back focal plane of the  $IL$ . In order to make the size of the source image equal to the pitch,  $p$ , of the MLA, the following equation must hold:

$$\phi_S = p \frac{f_{CL}}{f_{PL}}, \quad (6)$$

where  $f_{CL}$  and  $f_{PL}$  are the focal lengths of  $CL$  and  $IL$ , respectively. For the central element, it is easy to realize that the source image matches the central microlens. A simple ray tracing shows that the ray emerging from the center of  $S$ ,  $S_c$ , that crosses the  $CL$  at a height equal to the IMLA pitch (in  $P$ ) will pass through the center of the lenslet  $PL_{i+1}$  thus keeping its direction unchanged. As a result, this ray passes through the center of the element  $PL_{i+1}$  and the  $i + 1$  image of the source is coincident with the  $i + 1$  lenslet. Then, multiple images of  $S'$  are formed, each one being located onto an elemental cell in the PMLA.

Finally, we would like to emphasize that the optical barriers cannot be implemented by placing an array of light sources in front of the IMLA. Of course, in this case each source could be imaged at the center of the corresponding element in the PMLA with the proper size and location. However, the angular extension of the cone of rays that illuminates each elemental image would not be limited. Indeed, the light rays emerging from the  $i$ -th source would pass through the  $IL_{i+1}$  thus illuminating the  $i + 1$  elemental image. The paths of these rays will not be directed towards the center of the element  $PL_{i+1}$ , and some of them would pass through the element  $i + 2$  generating a pseudoimage.

## 5. Micro-Köhler integral imaging display

In this section we compare the performance of the proposed illumination system with the standard illumination system, showing that the flipping is indeed removed by our proposed system. The integral image was obtained from a virtual 3D scene using the 3DS MAX software. The virtual scene consisted of two identical cones at different depths from the microlens array, with the condition that the closest fits the FOV of the microlens centered at the optical axis. The elemental images were obtained by simulating an array of 50 x 50 cameras, each one having a FOV of 17.23 degrees and 33 mm of focal length, and a sensor of 10 mm x 10 mm and 35 pixels x 35 pixels. The distance (pitch) between cameras was 10 mm in both horizontal and vertical directions.

For the display the integral image was printed at a resolution of 600 dpi on a transparency for overhead projectors. The elemental image was scaled by a factor 10 to match a MLA with 3.3 mm of focal length and pitch of 1 mm. The scaling was homogeneous in order to avoid distortions on the reconstructed scene.

In the standard projection system we used a white-light bulb-lamp and a diffuser on the back side of an expander lens to provide the illumination. The observer was a Canon EOS 500D camera placed at a distance  $D = 550$  from the MLA, which we move horizontally and vertically from a point centered in the display. The maximum angular displacement was  $12^\circ$  in each direction. In Fig. 6, we show six views registered by the observer for each one. In this figure, we have prepared two movies in which we show frame by frame set of images captured in each direction.

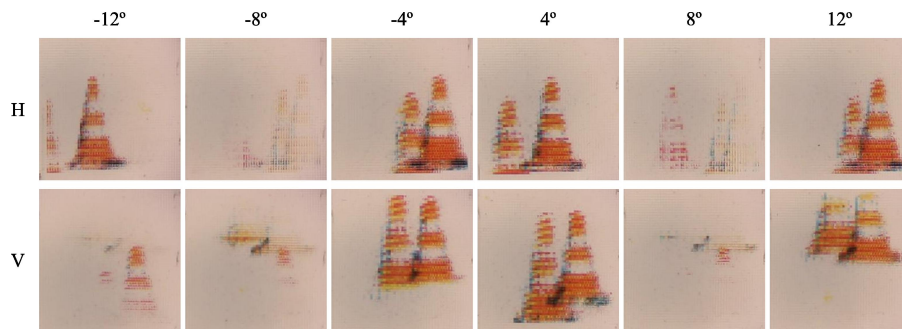


Fig. 6. The flipping effect is characteristic of conventional InIm displays. The top row shows different views for a horizontal (H) displacement of the observer ([Media 1](#)), and the lower a vertical (V) displacement ([Media 2](#)).

The first row shows the images seen when the observer moves horizontally between  $-12^\circ$  and  $12^\circ$ , i.e., from left to right. The central images ( $-4^\circ$ ,  $4^\circ$ ) correspond to images within the FOV of the 3D display: The parallax between the cones at the different depths is apparent. As the half FOV of the system was  $8^\circ$ , the images taken from this angle appear mixed. In the case of the image at  $-8^\circ$ , the cone on the left side of the image is reconstructed in its actual location. The other cone was out of the field of view. A new pair of cones starts to appear on the right side as a result of the flipping effect. These flipped cones are more noticeable for bigger angles, and the whole flipped image can be seen at  $-12^\circ$ . Note that this image is very similar to the one at  $4^\circ$ . The same effect happens when the observer moves towards positive angular deviations. When the observer moves in the vertical direction, we show the results in the second row in Fig. 6. The corresponding movie shows the effect of the flipping when the observer is moving between  $-12^\circ$  and  $12^\circ$ .

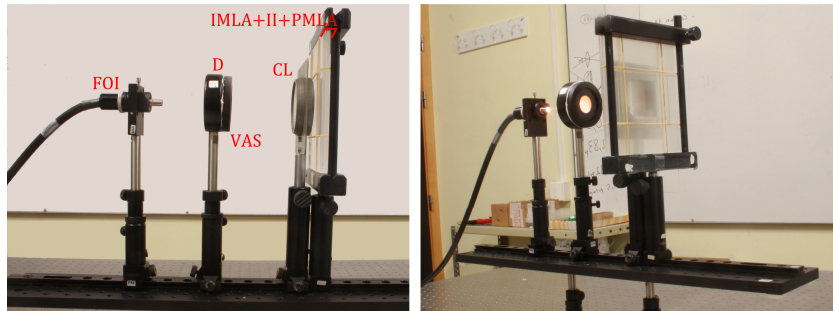


Fig. 7. Experimental micro-Köhler projection system shown from two different directions.

In the experimental implementation of the proposed multi-Köhler projector shown in Fig. 7, a fiber optic illumination (FOI) is adapted to illuminate the diffuser (D). At the back of the diffuser, a variable aperture diaphragm (VAP) serves to adjust the size of the diffuser that is actually illuminated. Next, a collimating lens (CL) with 62 mm of diameter and focal length 95 mm is placed so that the diffuser is centered on its back-focal point. An IMLA, with the same geometry as the MLA used for the standard illumination system, is placed after the field lens in order to provide the multi-Köhler illumination. The slide with the integral image is attached to this IMLA and the PMLA is placed at the focal plane of the first MLA. Finally, the diffuser aperture is changed so that its image onto the imaging MLA matches the lenslet size. In Fig. 8 we show the images registered by the observer in the same way as in a conventional display shown in Fig. 6. As in the standard system, the cone objects are clearly shown within the FOV ( $-4^\circ$ ,  $4^\circ$ ). Note that the extension of the observed image is now limited by a round aperture. This limitation comes from the aperture of the collimating lens. Also, the image looks slightly darker than in the conventional case as the luminance of the FOI used for the proposed system is lower than the luminance of the bulb used in the standard setup. When the observer is located in the borders of the field of view ( $-8^\circ$ ,  $8^\circ$ ), there is no flipped image appearing. For angles higher than the FOV no image is seen at all, as expected.

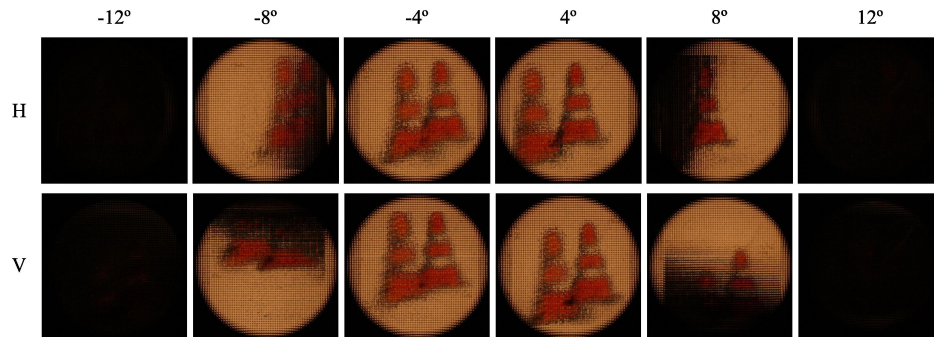


Fig. 8. The flipping effect is avoided when the multi-Köhler illumination is used. The top row shows different views for a horizontal (H) displacement of the observe ([Media 3](#)), and the lower a vertical (V) displacement ([Media 4](#)).

## 6. Conclusions

We have presented an all-optical technique to improve the FOV by avoiding the ghost images generated during the reconstruction also known as the flipping effect that is characteristic of conventional InIm displays. The system is based on the Köhler illumination concept. In addition, it provides a homogenous illumination source for the elemental images. The configuration proposed is optimal as it uses a single light-source and it is reconfigurable, as a change in the MLA characteristics simply implies a change in the size of the aperture diaphragm. The proposed technique is compared to the standard illumination system showing

its improved performance. This system is not compared with other methods found in the literature for avoiding flipping, as this comparison could be actually the subject of another paper. Two MLAs are needed to implement the system which is not a significant compromise as modern MLAs are relatively inexpensive and the alignment procedure is not complex. 3D display experiments have been presented to demonstrate the performance of the proposed setup. The proposed system can be used in a variety of integral imaging based 3D display systems [5–7].

### **Acknowledgments**

This work was supported in part by the Plan Nacional I + D + I, under Grants DPI2012-32994 and ENE2013-48565-C2-2-P, Ministerio de Economía y Competitividad (Spain), and also by the Generalitat Valenciana (Spain) under Grant PROMETEOII/2014/072. The work of Ángel Tolosa was supported by the Generalitat Valenciana under IVACE Grant PROMECE 2014.